



The Role of NaOH Content, Grinding Time, and Drying Temperature in Controlling the Shape and Size of Nano ZnO Synthesized by a Green Chemistry Approach



D. Refaat^{1,2*}, A.A. Farghali², A.A. Yousif³, M.G. Aggour⁴, M.H. Khedr²

¹Department of Pathology, Animal Health Research Institute (AHRI), Agricultural Research Center (ARC), Giza 12618, Egypt.

²Department of Materials Science and Nanotechnology, Faculty of Postgraduate Studies for Advanced Sciences (PSAS), Beni-Suef University, Beni-Suef 62511, Egypt.

³Department of Virology, Faculty of Veterinary Medicine, Cairo University, Giza, 12211, Egypt.

⁴Department of Biotechnology, Animal Health Research Institute (AHRI), Agricultural Research Center (ARC), Giza 12618, Egypt.

ZINC oxide (ZnO) has been widely exploited in different technological applications in virtue of its unique physical and chemical qualities. This study was designed to prepare ZnO nanorods for diagnostic applications using a simple, low cost, and solvent-deficient method with clarifying the effect of different experimental parameters on the shape and the size of the ZnO product. Under different experimental conditions, the synthesis was performed via a solid-state reaction of zinc sulfate and sodium hydroxide using the grinding method. The purity of nano ZnO products was investigated by X-ray diffractometer (XRD) while the size and the shape were demonstrated by high-resolution transmission electron microscopy (HRTEM). The XRD results confirmed the production of pure ZnO nanocrystals. The HRTEM micrographs illustrated the preparation of a mixture of nanospheroids and nanorods particles, nanorods with minor nanospheroids particles, and long nanorods particles when the applied mole ratio of (ZnSO₄·7H₂O: NaOH) was (1:2), (1:4), and (1:8) respectively. Our findings confirmed the vital role of NaOH in controlling the shape and the particle size of nano ZnO. Since ZnO nanorods can be easily prepared under mild environmentally friendly conditions, it is proposed that the described experimental conditions can be adapted for large scale production.

Keywords: Zinc oxide, Nanocrystals, NaOH, Grinding time, Drying temperature.

Introduction

Quite recently, nano ZnO has been considered as a key technological species [1] in virtue of their exclusive physical and chemical properties [2-5], such as unique optical properties [6], high electromechanical coupling that gives rise to efficient piezoelectric and pyroelectric properties [7], and diverse functionalities [8]. These merits foster the use of nano ZnO in optoelectronics [9], piezoelectric nanogenerators [10-12],

photocatalysis [13-15], and photonics such as UV-photodetectors [16], light-emitting diodes [17], and UV laser [18]. In the medical sectors, ZnO nanostructures have been widely applied as luminescent oxides [19], fluorescent fluorophores for cell labeling and imaging [20, 21] (including cancer cell probes [22, 23]), chemical sensors [24-28], in antimicrobial materials [29-34], and different nanomaterials for drug delivery [35] and gene therapy [36].

*Corresponding author: e-mail: [vet_dr_doaareffat@yahoo.com](mailto:veter_dr_doaareffat@yahoo.com)

Received 19/12/2019; Accepted 4/3/2020

DOI: 10.21608/ejchem.2020.21089.2264

©2020 National Information and Documentation Center (NIDOC)

Tuning the shape and the size of ZnO nanostructures is a prerequisite to the success of the targeted application [37-39]. ZnO has a unique capacity to grow in one-dimensional (1D), two-dimensional, and three-dimensional structures. 1D nanostructures include nanorods [40, 41], nanotubes [41, 42], nanowires [43, 44], nanoneedles [45], nanoribbons [46], and nanobelts [47]. ZnO 1D-nanostructures have attracted the attention of most researchers in virtue of their advantageous features mainly fewer defects related structure [48] and many attractive anisotropy-related characters that not easy to be achieved by size-tuning of their spherical counterparts. For instance, different ZnO nanocrystals (e.g. quantum dots, nanorods, and nanowires) have been applied in cancer detection and cell imaging [43, 49]. Additionally, Zhao *et al.* [50] illustrated the higher intensity of fluorescent signals in the case of nanorods in comparison with nanospheres, thus making them better candidates for biomolecule detection [51, 52]. There are various methods to produce ZnO nanorods such as; catalyst-free chemical vapor deposition (CVD) method [53], CVD method [54], hydrothermal synthesis [55], thermal evaporation technique [56], and mechanochemical (grinding) method [57]. However, most of the aforementioned methods are generally complicated and expensive [57, 58]. The grinding method is typically simple, cheap, suitable for large-scale production and environmentally friendly method.

For the best of our knowledge, there are few reports describing the preparation of nano ZnO using such a method. Additionally, most of these reports revealed the applying of high temperatures [59-61] and/or chemical additives either capping agents [62] or surfactants [58, 63, 64] that may induce some obstacles such as consuming high energy and existence of chemical impurities. Moreover, there are no sufficient studies exploring the role of the grinding experiment's parameters in controlling the shape and the size of nano ZnO. Therefore, the purpose of the present study is to synthesis ZnO nanorods using the grinding method and to investigate the effect of different experiment's conditions on the shape and the size of nano ZnO.

Materials and Methods

All of the reagents applied in this study were of analytical grades and were used without further purification. Zinc sulfate heptahydrate ($\text{ZnSO}_4 \cdot 7\text{H}_2\text{O}$) and sodium hydroxide pellets

(NaOH) were purchased from Molekula Company (UK). Absolute ethanol was purchased from Merck KGaA Company (Germany).

Mechanochemical synthesis

ZnO nanocrystals were synthesized according to Gautam *et al.* [65] with some modifications in the mole ratio of reactants, grinding times, and drying temperatures. Experiment (I); in three agate mortars, $\text{ZnSO}_4 \cdot 7\text{H}_2\text{O}$ (5.75 g, 0.02 mol) was put in such one with continuous grinding for 15 min. At room temperature, a subsequent mixing with NaOH pellets (1.59 g, 0.04 mol), (3.199 g, 0.08 mol) and (6.399g, 0.16 mol) took place respectively. Each mixture was then ground for 50 min. The outcome was washed and centrifuged at 6000 rpm (K centrifuge, TAIWAN) several times with deionized water (D.W.) then with absolute ethanol to get rid of the whole supernatant containing all contaminants. Finally, the end products were air-dried at room temperature then in a hot air oven (Venticell, Germany) at 120°C for four hours. To investigate the effects of grinding durations and drying temperatures on the synthesis of ZnO nanorods, experiment (II) was carried out as follows. In several agate mortars, $\text{ZnSO}_4 \cdot 7\text{H}_2\text{O}$ (5.75 g, 0.02 mol) was put in such one with continuous grinding for 15 min then each preparation was ground with NaOH pellets (3.199 g, 0.08 mol) for 50 min or 100 min at room temperature. The washing and air drying procedures were carried out as described before at room temperature. Subsequent drying at (180°C) or (120°C) in hot air oven was performed. Different conditions of synthesis and samples' key are shown in table 1.

Characterization:

The purity of the ZnO powders was estimated using XRD (Panalytical Empyrean, Netherland) using copper $\text{CuK}\alpha$ radiation ($\lambda=0.15406$ nm) in the range of 50-800 with a step size 0.04. The shape and the particles' size were examined using HRTEM (JEM-200100- JEOL, Japan).

Results and Discussion

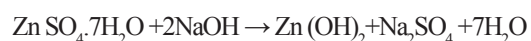
XRD patterns of samples (a), (z), (i), (g), (f), and (h) are shown in Fig. 1 and 2. All of the diffraction peaks were indexed using standard XRD data of ZnO (PDF cards no. 04-007-9805), (PDF cards no. 01-080-3004), (PDF cards no. 04-008-2750), (PDF cards no. 04-005-5076), (PDF cards no. 04-020-9583), (PDF cards no. 01-080-7099) respectively. The XRD patterns of all noted samples are compatible with the

TABLE 1. Different conditions of synthesis.

Sample Key	ZnSO ₄ .7H ₂ O: NaOH (mole ratio)	Grinding period (min)		Drying temperature (°C)	
		50	100	120	180
(a)	1:2	√	-	√	-
(z)	1:4	√	-	√	-
(g)	1:4	√	-	-	√
(h)	1:4	-	√	-	√
(f)	1:4	-	√	√	-
(i)	1:8	√	-	√	-

hexagonal wurtzite crystal structure of the standard XRD pattern of ZnO and no peaks for impurities indicating the production of pure ZnO nanocrystals. In Fig. 1, the intensity of XRD peaks increases by the increase of NaOH content revealing the increment of crystallinity while no significant changes can be observed in case of the noted samples (g), (f), and (h) as shown in Fig. 2 where NaOH content was the same.

This paper discusses the effects of precursors' different mole ratios, different grinding times, and drying temperatures on the particle size and shape of nano ZnO. Fig. 3-a shows the production of a mix of dominant nanospheroid particles with minor nanorods upon the use of (ZnSO₄.7H₂O: NaOH) at a mole ratio (1:2). By changing the mole ratio of (ZnSO₄.7H₂O: NaOH) to 1:4, the nanorods became the predominant nanostructure with the presence of minor nanospheroid particles (Fig. 3-z) that completely changed into pure long rod-shaped particles upon the use of (ZnSO₄.7H₂O: NaOH) at a mole ratio 1:8 (Fig. 3-i). These findings are in agreement with the results obtained by Hou et al. [57]. To interpret these results, it should first refer to the expected chemical equation explaining the reaction route of the ground precursors:



The previous equation showed the preparation of zinc hydroxide [66] while Zeferino et al. [67] recorded the direct production of tetrahydroxozincate [Zn(OH)₄]²⁻ in highly basic condition (abundant NaOH). In solid-state reaction, the phase transition or what is called phase transformation (crystal growth) was illustrated by Mnyukh [68]. He stated that "contact mechanism proceeds by the edgewise molecule-by-molecule formation of layers and layer-by-layer additions to the natural crystal face". Many studies demonstrated the effect of the basic content on the growth mechanism and the properties of ZnO nanoparticle [69, 70]. It has been established that adjusting the molar ratio of hydroxyl ions and zinc ions controls the preparation of ZnO with one-dimensional nanosized diameters [71]. Kawano and Imai [72] demonstrated the steep adsorption of [Zn(OH)₄]²⁻ on the (001) plane under high basic condition enhancing the growth along C axis giving rod shape. Complete conversion to zinc oxide occurs during the drying step using a hot air oven (equations 1&2). It is expected that partial conversion occurs during grinding step as a result of heat released by the grinding process itself [66, 67] and by NaOH as an exothermic substance. Concerning the size, the current results revealed the increase in the growth rate of rod-shaped particles by increasing NaOH that reached their maximum length when the mole ratio of

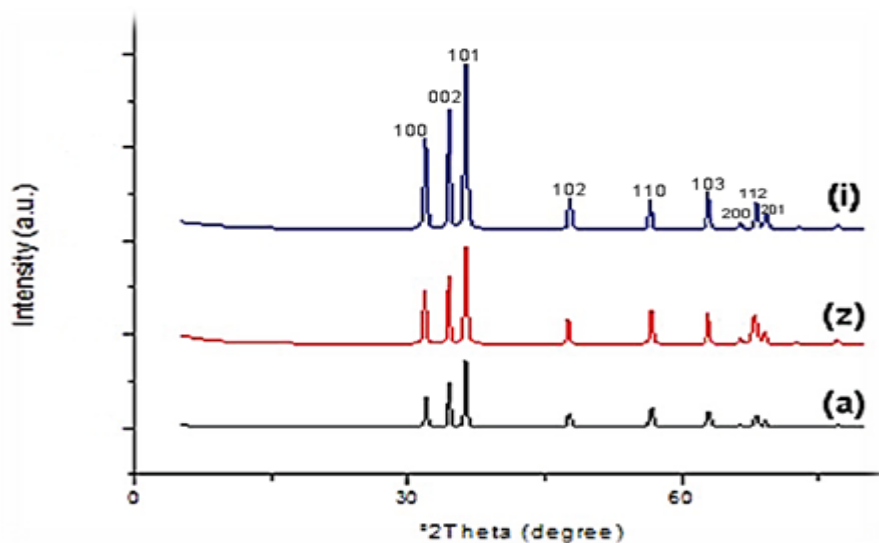


Fig. 1. XRD of samples (a), (z), and (i).

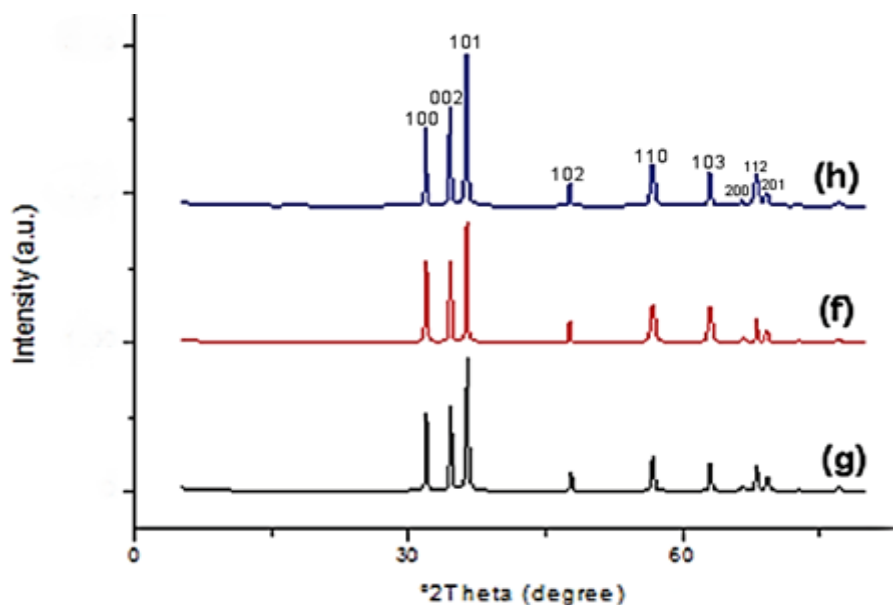
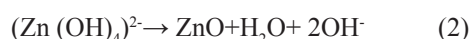


Fig. 2. XRD of samples (g), (f), and (h).

($\text{ZnSO}_4 \cdot 7\text{H}_2\text{O}$: NaOH) was 1:8. Zeferino *et al.* [67] explained that the increase in NaOH in the reaction mix causes a decrease in surface tension that in turn fostering the growth rate of ZnO.



The effect of the grinding times and drying temperatures on the shape and the particle size of nano ZnO are shown in Fig. 3z, 3g, 3f, and 3h. The results revealed no significant effect on the

shape or particle size of nano ZnO. Regarding the grinding time's effect; the present results are in contrast to results obtained by Dhara and Giri [73] and Salah *et al.* [74] that revealed the decrease in the particle size by increasing the milling reaction time. Elucidation of this contrast can be based on one of the two following assumptions; the first assumption is that long-time grinding produces smaller particles with higher surface areas, the high surfaced particles tend to agglomerate producing larger ones [75] due to Van der Waals

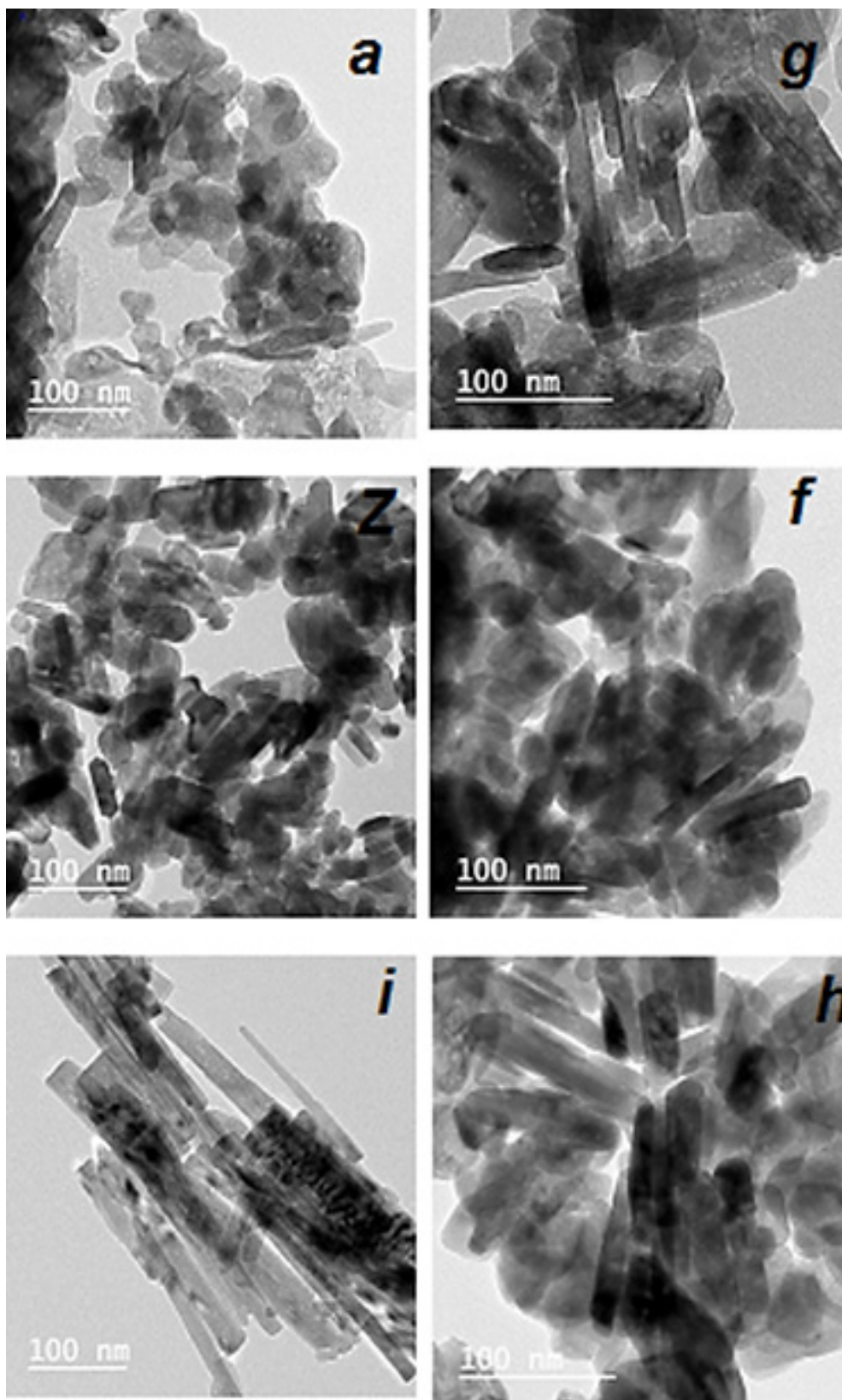


Fig. (3): HRTEM of samples (a), (z), (i), (g), (f), and (h)

or other attractive forces. On the other hand, according to results obtained by Nursyahadah *et al.* [76], we assume that grinding for 100 min may exceed the critical grinding time at which the crystallite size starts to increase in size due to cold welding.

As for the effect of drying temperatures; our results are incompatible with results obtained by Ao *et al.* [77], Sharma *et al.* [78], and GEMTA *et al.* [79] in which their results revealed the increase in the particle size by increasing the heat treatment. This contrast can be explained according to what was cited by Shaziman *et al.* [80] as follows. The high temperature may direct the movement of both atoms and molecules to be more violent which in turn deteriorates the crystal lattice's perfection resulting in rod particles' growth retardation. Furthermore, this contrast can be also attributed to the effect of different experimental conditions of such study. In an interesting comparative study performed by de Medeiros Machado *et al.* [81], it was shown that the effect of high temperature on the size of nano-ZnO varied according to the applied zinc precursor. More detailed research on the efficiency of the present ZnO nanorods product as fluorescent fluorophore to be applied in diagnostic field is currently in progress.

Conclusion

The present investigation shows the vital role of NaOH in controlling the morphology and the particle size of ZnO nanoproductions in comparison with different grinding times and /or drying temperatures. Additionally, either long grinding time or high drying temperature has no apparent effect on the shape or the size of nano ZnO particles. ZnO nanorods for a future application can be synthesized using a simple method under mild conditions with no need for organic solvents that overall complying the industrial production.

Acknowledgment

This research was financially supported by Science & Technology Development Fund (STDF)-Egypt, under Project No. 25343.

References

1. Parihar V, Raja M, Paulose R, A brief review of structural, electrical and electrochemical properties of zinc oxide nanoparticles. *Reviews on Advanced Materials Science*, 53(2), 119-30(2018).
2. Lucas E, Decker S, Khaleel A, Seitz A, Fultz S, Ponce A, *et al.*, Nanocrystalline metal oxides as unique chemical reagents/sorbents. *Chemistry–A European Journal*, 7(12), 2505-10(2001).
3. Srivastava V, Gusain D, Sharma YC, Synthesis, characterization and application of zinc oxide nanoparticles (n-ZnO). *Ceramics International*, 9803-8(2013).
4. Kumar H, Rani R, Structural and optical characterization of ZnO nanoparticles synthesized by microemulsion route. *International Letters of Chemistry, Physics, and Astronomy*, (14)26-36(2013).
5. Chey CO. Synthesis of ZnO and transition metals doped ZnO nanostructures, their characterization and sensing applications: Linköping University Electronic Press; 2014.
6. Yang P, Yan H, Mao S, Russo R, Johnson J, Saykally R, *et al.*, Controlled growth of ZnO nanowires and their optical properties. *Advanced functional materials*, 12(5), 323-31(2002).
7. Janotti A, Van de Walle CG, Fundamentals of zinc oxide as a semiconductor. *Reports on progress in physics*, 72(12), 126501(2009).
8. Vaseem M, Umar A, Hahn Y-B. ZnO nanoparticles: growth, properties, and applications. Metal oxide nanostructures and their applications. 5: American Scientific Publishers; 2010. p. 1-36.
9. Huang MH, Mao S, Feick H, Yan H, Wu Y, Kind H, *et al.*, Room-temperature ultraviolet nanowire nanolasers. *science*, 292(5523), 1897-9(2001).
10. Wang ZL, Song J, Piezoelectric nanogenerators based on zinc oxide nanowire arrays. *Science*, 312(5771), 242-6(2006).
11. Wang X, Song J, Liu J, Wang ZL, Direct-current nanogenerator driven by ultrasonic waves. *Science*, 316(5821), 102-5(2007).
12. Xu S, Qin Y, Xu C, Wei Y, Yang R, Wang ZL, Self-powered nanowire devices. *Nature nanotechnology*, 5(5), 366(2010).
13. Pyne S, Sahoo GP, Bhui DK, Bar H, Sarkar P, Samanta S, *et al.*, Enhanced photocatalytic activity of metal coated ZnO nanowires. *Spectrochimica Acta Part A: Molecular and Biomolecular Spectroscopy*, (93)100-5(2012).
14. Khalafi T, Buazar F, Ghanemi K, Phycosynthesis and enhanced photocatalytic activity of zinc oxide nanoparticles toward organosulfur pollutants. *Scientific reports*, 9(1), 1-10(2019).
15. Saleh SM, ZnO nanospheres based simple

- hydrothermal route for photocatalytic degradation of azo dye. *Spectrochimica Acta Part A: Molecular and Biomolecular Spectroscopy*, 211(141-7)(2019).
16. Lu C-Y, Chang S-J, Chang S-P, Lee C-T, Kuo C-F, Chang H-M, et al., Ultraviolet photodetectors with ZnO nanowires prepared on ZnO: Ga/glass templates. *Applied physics letters*, 89(15), 153101(2006).
 17. Na JH, Kitamura M, Arita M, Arakawa Y, Hybrid p-n junction light-emitting diodes based on sputtered ZnO and organic semiconductors. *Applied Physics Letters*, 95(25), 329(2009).
 18. Chu S, Wang G, Zhou W, Lin Y, Chernyak L, Zhao J, et al., Electrically pumped waveguide lasing from ZnO nanowires. *Nature nanotechnology*, 6(8), 506(2011).
 19. Li J, Fan H, Jia X, Chen J, Cao Z, Chen X, Electrostatic spray deposited polycrystalline zinc oxide films for ultraviolet luminescence device applications. *Journal of Alloys and Compounds*, 481(1-2), 735-9(2009).
 20. Xiong H-M, Xu Y, Ren Q-G, Xia Y-Y, Stable aqueous ZnO@polymer core-shell nanoparticles with tunable photoluminescence and their application in cell imaging. *Journal of the American Chemical Society*, 130(24), 7522-3(2008).
 21. Zang Z, Tang X, Enhanced fluorescence imaging performance of hydrophobic colloidal ZnO nanoparticles by a facile method. *Journal of Alloys and Compounds*, 619(98-101)(2015).
 22. Sudhagar S, Sathya S, Pandian K, Lakshmi BS, Targeting and sensing cancer cells with ZnO nanoprobes in vitro. *Biotechnology letters*, 33(9), 1891-6(2011).
 23. Hong H, Wang F, Zhang Y, Graves SA, Eddine SBZ, Yang Y, et al., Red fluorescent zinc oxide nanoparticle: a novel platform for cancer targeting. *ACS applied materials & interfaces*, 7(5), 3373-81(2015).
 24. Wei A, Sun XW, Wang J, Lei Y, Cai X, Li CM, et al., Enzymatic glucose biosensor based on ZnO nanorod array grown by hydrothermal decomposition. *Applied Physics Letters*, 89(12), 123902(2006).
 25. Zang J, Li CM, Cui X, Wang J, Sun X, Dong H, et al., Tailoring zinc oxide nanowires for high performance amperometric glucose sensor. *Electroanalysis: An International Journal Devoted to Fundamental and Practical Aspects of Electroanalysis*, 19(9), 1008-14(2007).
 26. Ansari AA, Singh R, Sumana G, Malhotra B, Sol-gel derived nano-structured zinc oxide film for sexually transmitted disease sensor. *Analyst*, 134(5), 997-1002(2009).
 27. Galstyan V, Comini E, Baratto C, Faglia G, Sberveglieri G, Nanostructured ZnO chemical gas sensors. *Ceramics International*, 41(10), 14239-44(2015).
 28. Agarwal S, Rai P, Gatell EN, Llobet E, Güell F, Kumar M, et al., Gas sensing properties of ZnO nanostructures (flowers/rods) synthesized by hydrothermal method. *Sensors and Actuators B: Chemical*, (292)24-31(2019).
 29. Mirhosseini M, Firouzabadi FB, Antibacterial activity of zinc oxide nanoparticle suspensions on food-borne pathogens. *International Journal of Dairy Technology*, 66(2), 291-5(2013).
 30. Shi L-E, Li Z-H, Zheng W, Zhao Y-F, Jin Y-F, Tang Z-X, Synthesis, antibacterial activity, antibacterial mechanism and food applications of ZnO nanoparticles: a review. *Food Additives & Contaminants: Part A*, 31(2), 173-86(2014).
 31. Podporska-Carroll J, Myles A, Quilty B, McCormack DE, Fagan R, Hinder SJ, et al., Antibacterial properties of F-doped ZnO visible light photocatalyst. *Journal of hazardous materials*, 324(39-47)(2017).
 32. Khan MF, Ansari AH, Hameedullah M, Ahmad E, Husain FM, Zia Q, et al., Sol-gel synthesis of thorn-like ZnO nanoparticles endorsing mechanical stirring effect and their antimicrobial activities: Potential role as nano-antibiotics. *Scientific reports*, 6(27689)(2016).
 33. Jin S-E, Jin JE, Hwang W, Hong SW, Photocatalytic antibacterial application of zinc oxide nanoparticles and self-assembled networks under dual UV irradiation for enhanced disinfection. *International journal of nanomedicine*, 14(1737)(2019).
 34. Ogunyemi SO, Abdallah Y, Zhang M, Fouad H, Hong X, Ibrahim E, et al., Green synthesis of zinc oxide nanoparticles using different plant extracts and their antibacterial activity against *Xanthomonas oryzae* pv. *oryzae*. *Artificial cells, nanomedicine, and biotechnology*, 47(1), 341-52(2019).
 35. Leone F, Cataldo R, Mohamed SS, Manna L,

- Banchero M, Ronchetti S, et al., Nanostructured ZnO as multifunctional carrier for a green antibacterial drug delivery system—A feasibility study. *Nanomaterials*, 9(3), 407(2019).
36. Zhang Y, R Nayak T, Hong H, Cai W, Biomedical applications of zinc oxide nanomaterials. *Current molecular medicine*, 13(10), 1633-45(2013).
37. Raula M, Rashid MH, Paira TK, Dinda E, Mandal TK, Ascorbate-assisted growth of hierarchical ZnO nanostructures: sphere, spindle, and flower and their catalytic properties. *Langmuir*, 26(11), 8769-82(2010).
38. Rai P, Jo J-N, Lee I-H, Yu Y-T, Fabrication of flower-like ZnO microstructures from ZnO nanorods and their photoluminescence properties. *Materials Chemistry and Physics*, 124(1), 406-12(2010).
39. Davis K, Yarbrough R, Froeschle M, White J, Rathnayake H, Band gap engineered zinc oxide nanostructures via a sol-gel synthesis of solvent driven shape-controlled crystal growth. *RSC advances*, 9(26), 14638-48(2019).
40. Yi G-C, Wang C, Park WI, ZnO nanorods: synthesis, characterization and applications. *Semiconductor Science and Technology*, 20(4), S22(2005).
41. Song J, Lim S, Effect of seed layer on the growth of ZnO nanorods. *The Journal of Physical Chemistry C*, 111(2), 596-600(2007).
42. Zhang B, Binh N, Wakatsuki K, Segawa Y, Yamada Y, Usami N, et al., Formation of highly aligned ZnO tubes on sapphire (0001) substrates. *Applied Physics Letters*, 84(20), 4098-100(2004).
43. Hong H, Shi J, Yang Y, Zhang Y, Engle JW, Nickles RJ, et al., Cancer-targeted optical imaging with fluorescent zinc oxide nanowires. *Nano letters*, 11(9), 3744-50(2011).
44. Xu F, Shen Y, Sun L, Zeng H, Lu Y, Enhanced photocatalytic activity of hierarchical ZnO nanoplate-nanowire architecture as environmentally safe and facily recyclable photocatalyst. *Nanoscale*, 3(12), 5020-5(2011).
45. Park WI, Yi GC, Kim M, Pennycook SJ, ZnO nanoneedles grown vertically on Si substrates by non-catalytic vapor-phase epitaxy. *Advanced Materials*, 14(24), 1841-3(2002).
46. Yan H, Johnson J, Law M, He R, Knutsen K, McKinney JR, et al., ZnO nanoribbon microcavity lasers. *Advanced Materials*, 15(22), 1907-11(2003).
47. Ding Y, Zhang F, Wang ZL, Deriving the three-dimensional structure of ZnO nanowires/nanobelts by scanning transmission electron microscope tomography. *Nano Research*, 6(4), 253-62(2013).
48. Chakrabarti S, Chaudhuri S, Microstructural and photoluminescent characterization of one-dimensional ZnO nanostructures prepared by catalyst-assisted vapour-liquid-solid technique. *Materials chemistry and physics*, 87(1), 196-200(2004).
49. Zhang H, Chen B, Jiang H, Wang C, Wang H, Wang X, A strategy for ZnO nanorod mediated multi-mode cancer treatment. *Biomaterials*, 32(7), 1906-14(2011).
50. Zhao Y, Wang Y, Ran F, Cui Y, Liu C, Zhao Q, et al., A comparison between sphere and rod nanoparticles regarding their in vivo biological behavior and pharmacokinetics. *Scientific reports*, 7(1), 4131(2017).
51. Nath N, Chilkoti A, Label-free biosensing by surface plasmon resonance of nanoparticles on glass: optimization of nanoparticle size. *Analytical Chemistry*, 76(18), 5370-8(2004).
52. Orendorff CJ, Gole A, Sau TK, Murphy CJ, Surface-enhanced Raman spectroscopy of self-assembled monolayers: sandwich architecture and nanoparticle shape dependence. *Analytical chemistry*, 77(10), 3261-6(2005).
53. Wu J-J, Liu S-C, Catalyst-free growth and characterization of ZnO nanorods. *The Journal of Physical Chemistry B*, 106(37), 9546-51(2002).
54. Wu JJ, Liu SC, Low-temperature growth of well-aligned ZnO nanorods by chemical vapor deposition. *Advanced materials*, 14(3), 215-8(2002).
55. Sun X, Chen X, Deng Z, Li Y, A CTAB-assisted hydrothermal orientation growth of ZnO nanorods. *Materials Chemistry and Physics*, 78(1), 99-104(2003).
56. Hu P, Han N, Zhang D, Ho JC, Chen Y, Highly formaldehyde-sensitive, transition-metal doped ZnO nanorods prepared by plasma-enhanced chemical vapor deposition. *Sensors and Actuators B: Chemical*, 169(74-80)(2012).
57. Hou X, Zhou F, Liu W, A facile low-cost synthesis of ZnO nanorods via a solid-state

- reaction at low temperature. *Materials Letters*, 60(29-30), 3786-8(2006).
58. Sun Z-P, Liu L, Zhang L, Jia D-Z, Rapid synthesis of ZnO nano-rods by one-step, room-temperature, solid-state reaction and their gas-sensing properties. *Nanotechnology*, 17(9), 2266(2006).
59. Azam A, Ahmed F, Arshi N, Chaman M, Naqvi A, Low temperature synthesis of ZnO nanoparticles using mechanochemical route: A green chemistry approach. *International Journal of Theoretical and Applied Sciences*, 1(2), 12-4(2009).
60. Zhang X, Qin J, Xue Y, Yu P, Zhang B, Wang L, et al., Effect of aspect ratio and surface defects on the photocatalytic activity of ZnO nanorods. *Scientific reports*, (4) 4596(2014).
61. Smith SJ, Huang B, Liu S, Liu Q, Olsen RE, Boerio-Goates J, et al., Synthesis of metal oxide nanoparticles via a robust "solvent-deficient" method. *Nanoscale*, 7(1), 144-56(2015).
62. Jitti-a-porn P, Suwanboon S, Amornpitoksuk P, Patarapaiboolchai O, Defects and the optical band gap of ZnO nanoparticles prepared by a grinding method. *Journal of Ceramic Processing Research*, 12(1), 85-9(2011).
63. Jin C-f, Yuan X, Ge W-w, Hong J-m, Xin X-q, Synthesis of ZnO nanorods by solid state reaction at room temperature. *Nanotechnology*, 14(6), 667(2003).
64. Vidyasagar C, Naik YA, Surfactant (PEG 400) effects on crystallinity of ZnO nanoparticles. *Arabian Journal of Chemistry*, 9(4), 507-10(2016).
65. Gautam M, Verma M, Misra G, Structural and optical properties of ZnO nanocrystals. *Journal of biomedical nanotechnology*, 7(1), 161-2(2011).
66. Zhu Y, Zhou Y, Preparation of pure ZnO nanoparticles by a simple solid-state reaction method. *Applied Physics A*, 92(2), 275-8(2008).
67. Zeferino RS, Ramón JAR, de Anda Reyes ME, Gonzalez NRS, Pal U, Large scale synthesis of ZnO nanostructures of different morphologies through solvent-free mechanochemical synthesis and their application in photocatalytic dye degradation. *American Journal of Engineering and Applied Sciences*, 9(1), 41-52(2016).
68. Mnyukh Y, Mechanism and kinetics of phase transitions and other reactions in solids. *arXiv preprint arXiv:11101654*, 2011).
69. Ram SG, Kulandainathan MA, Ravi G, On the study of pH effects in the microwave enhanced rapid synthesis of nano-ZnO. *Applied Physics A*, 99(1), 197-203(2010).
70. Amin G, Asif M, Zainelabdin A, Zaman S, Nur O, Willander M, Influence of pH, precursor concentration, growth time, and temperature on the morphology of ZnO nanostructures grown by the hydrothermal method. *Journal of Nanomaterials*, (5)(2011).
71. Li P, Wei Y, Liu H, Wang X, A simple low-temperature growth of ZnO nanowhiskers directly from aqueous solution containing Zn (OH) 4²⁻ ions. *Chemical Communications*, (24), 2856-7(2004).
72. Kawano T, Imai H, Fabrication of ZnO nanoparticles with various aspect ratios through acidic and basic routes. *Crystal growth & design*, 6(4), 1054-6(2006).
73. Dhara S, Giri P, Quick single-step mechanosynthesis of ZnO nanorods and their optical characterization: milling time dependence. *Applied Nanoscience*, 1(4), 165-71(2011).
74. Salah N, Habib SS, Khan ZH, Memic A, Azam A, Alarfaj E, et al., High-energy ball milling technique for ZnO nanoparticles as antibacterial material. *International journal of nanomedicine*, 6(863)(2011).
75. Momen G, Farzaneh M, Survey of micro/nano filler use to improve silicone rubber for outdoor insulators. *Rev Adv Mater Sci*, 27(1), 1-13(2011).
76. Nursyahadah M, Zakaria A, Singh Raman R, Venugopal T, Talari MK, editors. Effect of milling time on properties of mechanochemically synthesized nano ZnO. AIP Conference Proceedings; 2010: AIP.
77. Ao W, Li J, Yang H, Zeng X, Ma X, Mechanochemical synthesis of zinc oxide nanocrystalline. *Powder Technology*, 168(3), 148-51(2006).
78. Sharma J, Vashishtha M, Shah D, Crystallite size dependence on structural parameters and photocatalytic activity of microemulsion mediated synthesized ZnO nanoparticles annealed at different temperatures. *Global Journal of Science Frontier Research*, 14(5), 2014).
79. GEMTA AB, Bekele B, Reddy AC, Effects of Temperature and Polyvinyl Alcohol concentrations in the Synthesis of Zinc Oxide Nanoparticles. *Egypt. J. Chem.* 63, No. 10 (2020)

- Journal of Nanotechnology and Materials Science*, 5(1), 44-50(2018).
80. Shaziman S, Ismail AS, Mamat MH, Zoolfakar AS, editors. Influence of growth time and temperature on the morphology of ZnO nanorods via hydrothermal. IOP Conference Series: Materials Science and Engineering; 2015: IOP Publishing.
81. de Medeiros Machado M, Savi BM, Perucchi MB, Benedetti A, Oliveira LFS, Bernardin AM, Effect of Temperature, Precursor Type and Dripping Time on the Crystallite Size of Nano ZnO Obtained by One-Pot Synthesis: 2 k Full Factorial Design Analysis. *Nanoscience and Nanotechnology*, 17(1-4)(2017).

دور هيدروكسيد الصوديوم، مدة الطحن، ودرجة حرارة التجفيف في التحكم بشكل وحجم أكسيد الزنك النانوي المخلوق باستخدام الكيمياء الآمنة

دعاء رفعت^١، أحمد على^٢، أسامة عبد الرؤوف^٣، محمد جلال^٤، محمد خضر^٥

^١قسم الباثولوجيا، معهد بحوث الصحة الحيوانية، مركز البحوث الزراعية، مصر.

^٢قسم علوم المواد وتكنولوجيا النانو، كلية الدراسات العليا للعلوم المتقدمة، جامعة بنى سويف.

^٣قسم الفيرولوجي، كلية الطب البيطري، جامعة القاهرة.

^٤قسم البيوتكنولوجيا، معهد بحوث الصحة الحيوانية، مركز البحوث الزراعية، مصر.

لقد تم استخدام أكسيد الزنك حديثاً على نطاق تكنولوجي واسع لما يتميز به من خصائص فيزيائية وكيميائية فريدة. وتهدف الدراسة الحالية إلى تحضير جزيئات عسوية من أكسيد الزنك النانوي بغرض تطبيقه في مجال التشخيص الطبى وذلك باستخدام إحدى طرق التخليق البسيطة، منخفضة التكلفة، والتي لا تحتاج إلى استعمال مذيبات. كما تهدف الدراسة إلى توضيح تأثير العوامل التجريبية المختلفة على حجم وشكل جزيئات أكسيد الزنك. ولقد تمت عملية التخليق تحت ظروف معملية مختلفة من تفاعل كبريتات الزنك وهيدروكسيد الصوديوم باستخدام طريقة الطحن. ولقد تم فحص الجزيئات المتكونة من حيث درجة نقائها، حجمها وشكلها باستخدام كلا من اختبار «حيود الأشعة السينية» ومجهر النفاذ الإلكتروني عالي الدقة على التوالي. ولقد أكدت نتائج اختبار «حيود الأشعة السينية» إنتاج كريستالات أكسيد الزنك النانوية النقية. كما أوضح الفحص المجهرى تكون جزيئات نانوية شبه كروية وأخرى عسوية. جزيئات نانوية عسوية مع تواجد ضئيل لأخرى كروية الشكل. جزيئات عسوية طويلة وذلك عند استخدام (كبريتات الزنك: هيدروكسيد الصوديوم) بنسبة مولية (٢:١)، (٤:١)، (٨:١) على التوالي. تؤكد النتائج على الدور الهام لهيدروكسيد الصوديوم في التحكم بالحجم وشكل جزيئات أكسيد الزنك النانوية. ومن ثم فإنه يمكن تحضير جزيئات أكسيد الزنك النانوية العسوية في ظل ظروف تجريبية بسيطة وصديقة للبيئة تتناسب مع متطلبات الإنتاج على نطاق واسع.